GFZ

Helmholtz Centre
POTSDAM

HELMHOLTZ CENTRE POTSDAM
GFZ GERMAN RESEARCH CENTRE
FOR GEOSCIENCES

Shahid Ullah, Stefano Parolai, Massimiliano Pittore

A Report on Site Effects Studies in Kyrgyzstan

Scientific Technical Report STR16/02

www.gfz-potsdam.de

HELMHOLTZ
ASSOCIATION

Recommended citation:

Ullah, S., Parolai, S., Pittore, M. (2016): A report on site effects studies in Kyrgyzstan: recommendation for a new seismic normative, (Scientific Technical Report; 16/02), Potsdam: GFZ German Research Center for Geosciences.
DOI: http://doi.org/10.2312/GFZ.b103-1602en

A Russian translation of this report is available via:

Ullah, S., Parolai, S., Pittore, M. (2016): Отчет исследований сайт-эффектов в Кыргызстане, (Scientific Technical Report STR; 16/02), Potsdam: GFZ German Research Center for Geosciences.
DOI: http://doi.org/10.2312/GFZ.b103-1602ru

Переведенный отчет на русском языке доступен:

Ullah, S., Parolai, S., Pittore, M. (2016): Отчет исследований сайт-эффектов в Кыргызстане, (Scientific Technical Report STR; 16/02), Potsdam: GFZ German Research Center for Geosciences.
DOI: http://doi.org/10.2312/GFZ.b103-1602ru

Imprint

Helmholtz Centre Potsdam
GFZ German Research Centre for Geosciences

Telegrafenberg
D-14473 Potsdam

Published in Potsdam, Germany
January 2016

ISSN 2190-7110

DOI: http://doi.org/10.2312/GFZ.b103-1602en
URN: urn:nbn:de:kobv:b103-1602en2

This work is published in the GFZ series
Scientific Technical Report (STR)
and electronically available at GFZ website
www.gfz-potsdam.de

Shahid Ullah, Stefano Parolai, Massimiliano Pittore

A Report on Site Effects Studies in Kyrgyzstan

January 2016

Scientific Technical Report STR16/02

Mr. Shahid Ullah
Prof. Dr. Stefano Parolai
Dr. Massimiliano Pittore
Centre for Early Warning Systems
Helmholtz Centre Potsdam GFZ German Research Centre for Geosciences
Helmholtzstrasse 7
D-14467 Potsdam, Germany

Table of Contents

1 Introduction

Surface geology plays an important role in the spatial variability over short distance (also less than 1 km) of ground shaking during an earthquake. Recent earthquakes have shown that this aspect, generally referred to as site effects, plays an important role in defining the amount and spatial distribution of damage within urban areas. The identification of such factors (termed site effects) has been of interest in Central Asia, in particular the Kyrgyz Republic, and is a critical aspect of seismic hazard assessment, especially in urban areas (e.g., Pilz et al., 2015).

Figure 1 shows, in a schematic way, for the case of a shallow event over distances where the greatest amount of damage can be observed, the waves propagating through the crust and that due to the near surface geology results in the ground motion recordings at two stations (S1 and S2) being very different both in terms of duration and amplitude. In this case, S1 is placed on a rock site while S2, experiencing the highest level of ground motion, is located on soft unconsolidated sediments.

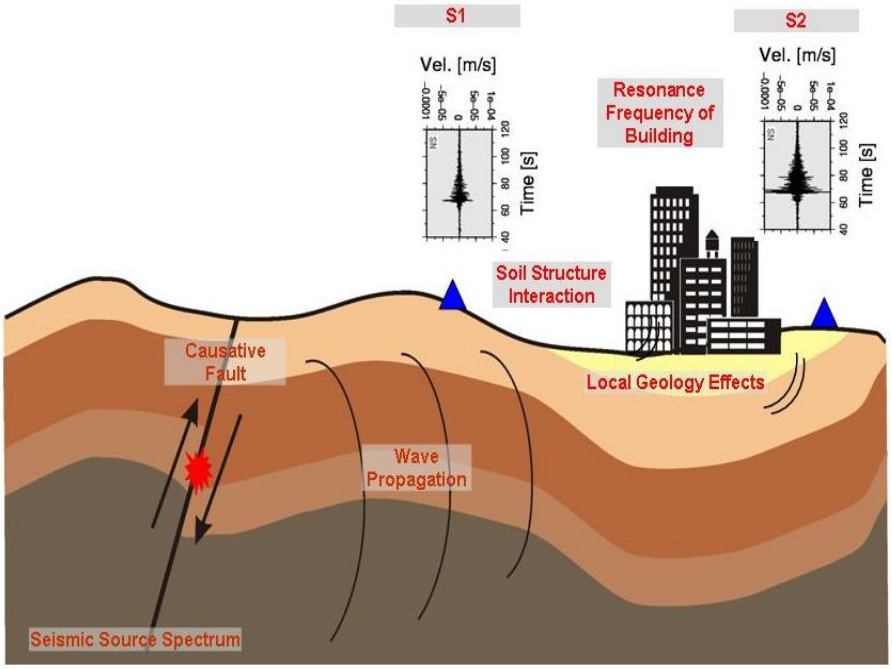

***Figure 1**: Simplified representation showing seismic wave propagation after an earthquake. Blue triangles indicate stations located over different near-surface geological material (S1 on a rock site and S2 on soft Quaternary material), hence experiencing different ground motion. (Bormann, 2012).*

The modification of ground motion (i.e., amplification, de-amplification at certain frequencies) depends on many factors, the most important of these being the depth of the sediments, the shear wave velocity of the sediments and the impedance contrast between the sediments and the underlying bedrock. The impedance contrast $c = (v_2\ \rho_2)/(v_1\ \rho_1)$, where ρ_1 and ρ_2 are the density and v_1 and v_1 are the wave propagation velocities in the sedimentary cover and bedrock, respectively, determines how strongly the waves at particular frequencies (especially the fundamental resonance frequency and the higher harmonics) are multi-reflected within the

soft layer, thus trapping the wave energy within the layer (1D effect). Quantitatively, and under the simplified assumption of vertical propagation of S-waves, the modulus of the 1D site amplification function $H(f)$ can be described by the following relation:

$$|H(f)| = \left(\frac{(1+r)^2}{1+2r\cos(4\pi f\tau)+r^2} \right)^{\frac{1}{2}} \qquad (1)$$

where τ is the travel time of the S-waves in the soft sedimentary layer and r=($\rho_2 v_2$-$\rho_1 v_1$)/($\rho_2 v_2$+$\rho_1 v_1$) is the reflection coefficient that is clearly related to the impedance contrast c. The maximum of $H(f)$ is obtained when $\cos(4\pi f\tau)$ is equal to -1, that is when f=1/(4τ). This value of f is defined as the fundamental resonance frequency f_0. From Equation 1 we obtain the well-known relationship f_0=v_1/(4h_1), where h1 is the thickness of the soft sedimentary layer.

Site effects can be estimated using numerical and empirical methods. Numerical methods require a detailed knowledge of properties of the sub-surface geology. The empirical methods are generally divided into two categories: 1) reference site methods, and 2) non-reference site methods. In reference site methods, i.e., standard spectral ratios (SSR), the ground motion recorded at two nearby sites is compared in the frequency domain. One site, which is considered as the reference site, is usually located on outcropping hard rock, and is assumed to have the same source and path effects as the other site. Hence the difference between the two sites is considered to be the local site effects. However, the disadvantage of this method is that a suitable reference site may not be easily available everywhere, while an inappropriate reference site may have its own site effects. To overcome this problem, non-reference site methods, i.e., horizontal to vertical spectral ratios (HV) are used, in which the horizontal component of ground motion is compared with vertical component for the same site in the frequency domain. Although non-reference site methods provide good estimates of the S-wave resonance frequency of sediments, they might underestimate the level of amplification with respect to reference site methods.

This report presents some results of site effects studies carried out in the Kyrgyz Republic by the Helmholtz Centre Potsdam German Research Centre for Geosciences, Potsdam, Germany (GFZ) and the Central Asian Institute for Applied Geosciences, Bishkek, Kyrgyz Republic (CAIAG). This work was carried out within the context of a number of projects, such as the Central Asian component of the Global Earthquake Model (GEM[1]) initiative (Earthquake Model Central Asia, EMCA[2]). Several papers related to this theme are included in an annex.

[1] http://www.globalquakemodel.org/
[2] http://www.emca-gem.org/

2 Site effects assessment

2.1 Bishkek

Site effects studies were carried out in Bishkek using reference and non-reference site techniques and combining earthquake and noise recording analysis results. Figure 2 shows the locations of 19 seismic stations that formed a temporary seismic network installed in 2008 to collect earthquake and seismic noise data, as well as the surface geology of the city, including the location of the main fault in the area. However, in order to obtain a more resolved understanding of the spatial variability in the site affects, seismic noise was recorded at about 200 locations (represented by solid circles in Figure 2) over short periods of about 30 minutes. Furthermore, seismic noise array measurements were carried out to estimate the S-wave velocity profile in different locations in the urban area. Station BI04, located in the Kyrgyz Range in the south, and was considered to be the reference site in the SSR analyses, although its H/V results depicted some amplifications at frequencies higher than 3-4 HZ (Parolai et al., 2010).

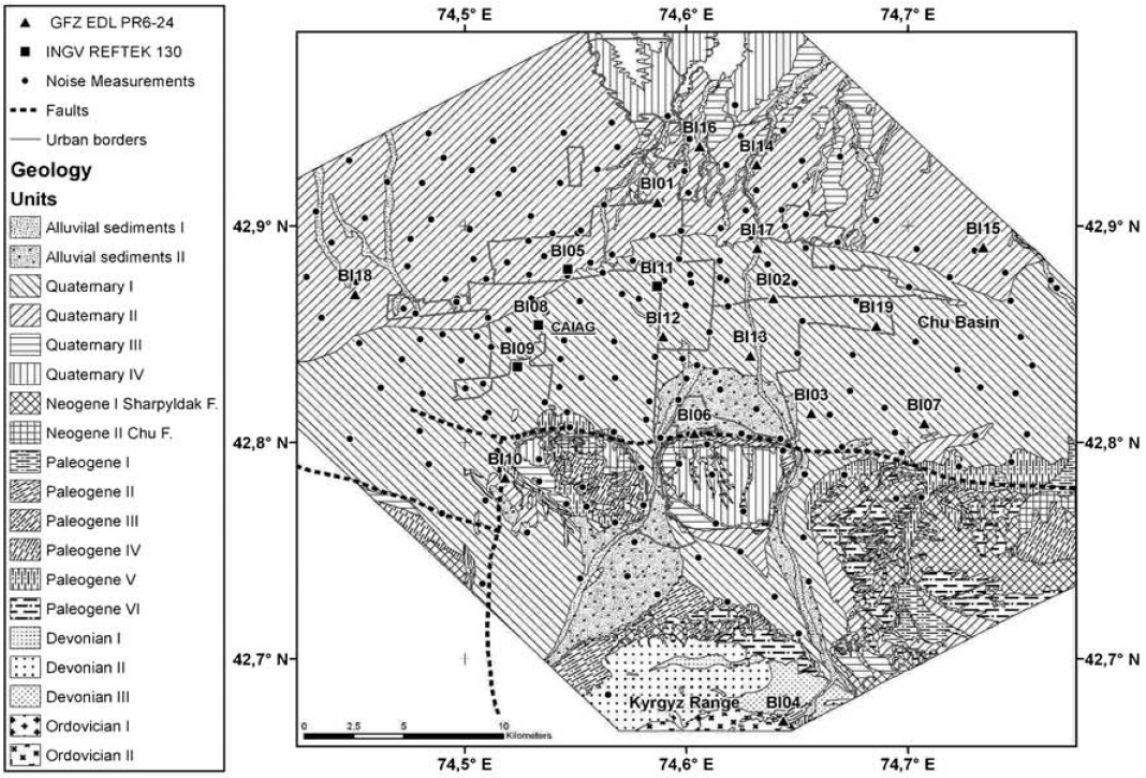

Figure 2: *Seismic network set-up in Bishkek, consisting of temporary seismic network (solid triangles and squares) and single station measuring points (solid circle) (Parolai et al., 2010).*

Figure 3 shows examples of the large amplification observed using different analysis methods at stations located in different positions within Bishkek. A complete and exhaustive analysis of the results is presented in Parolai et al. (2010), where the methods and data analysis are explained in details. Since the results are similar for both horizontal components of ground motion (east west and north south), the results are presented here only for the east-west components of the recordings. From the main results of the analysis carried (Parolai et al., 2010), it is worth highlighting:

1. The HVSR for the stations installed in the northern part of the town over the older Quaternary material clearly show a first resonant peak at ~0.2 Hz. After a narrow trough at around 0.3 Hz, the HVSR is almost flat and then shows a bump starting from between 2-3 Hz up to 10 Hz. The stations located in the central part of the urban area show a smaller-amplitude low-frequency peak (between 0.1 and 0.2 Hz) followed by a very large trough and then by a nearly flat HVSR. The stations located at the southern margin of the study area, where the Tertiary material makes a tectonic contact with the Quaternary sediments, show a peculiar behavior strongly dependent on small scale changes in the surface geology. Finally, it is worth noting that the HVSR at station BI04, which was supposed to be the reference station, can be considered flat only up to around 2 Hz. At higher frequencies, large amplifications are observed, with a prominent peak at ~ 5 Hz.
2. Although station BI04 was found to be not an ideal reference site, it was still used as a reference station for the frequency range lower than 2 Hz. In fact, over this range, the HVSR results show values of nearly one. Furthermore, the distance between this station and the other stations of the network is short enough to assume that only minor propagation effects are affecting the SSR results over this frequency range. Results obtained for the East-West (EW) and vertical (Z) components of ground motion are shown in Figure 3 (third column). Differently from the HVSR, results of all the stations in the basin show very similar behavior for the horizontal component SSR. In particular, a broad amplification is observed with clearly distinct peaks between 0.2 and 0.1 Hz (decreasing from North to South), 0.4 Hz and between 1 and 2 Hz. Occasionally, some stations also show distinct amplification peaks at 0.6-0.7 Hz. Above 2 Hz, the large de-amplification effect is due to the amplification occurring at the reference site. Stations located at the southern margin of the basin show different behaviors. In some cases, the site response was found to be nearly flat with a small amplification at around 1.5 Hz. In other cases, only moderate amplification was observed, increasing nearly linearly from the lower frequencies up to 1-2Hz. The following decaying trend is not reliable due to the amplification affecting the reference station over that frequency range. The differences between the HVSR and SSR results can be easily explained by considering the SSR results obtained by analyzing the vertical component of ground motion. In fact, the vertical component SSR of the stations within the basin (Figure 3, fourth column) are showing large amplifications with peaks at frequencies (~0.3-0.5 Hz) systematically larger than those observed on the horizontal component results. These peaks are particularly large, even occasionally becoming predominant, for the stations BI13, BI08, BI09, BI11 located on the younger Quaternary sediments outcropping in the southern part of the urban area. The positions of these peaks coincide with the spectral troughs in the HVSR. Considering that the HVSR of the reference station is not affected by the narrow spectral troughs at 0.3-0.5 Hz (indicating that no amplification of the vertical component in that frequency range take place outside of the basin), and that the role of surface waves might be ruled out since the amplitude peaks in the

lower frequency range are occurring at different frequencies on the vertical and horizontal components, the results might be interpreted by considering the effect of converted waves on the recorded ground motion. In fact, previous studies (e.g., Takahashi et al., 1992; Parolai and Richwalski, 2004) showed that at the boundaries between shallow geological layers, significant P-to-S and S-to-P conversion can take place and, therefore affect the HVSR results.

3. A generally good agreement between the fundamental frequency of resonance obtained from the HVSR (first column) and the NHVSR (second column) is observed. The results presented in Figure 4 show that in the urban area of Bishkek, north of the outcropping Tertiary material, the fundamental resonance frequency of soil spans, consistent with the SSR results, from nearly 0.3 Hz in the North to ~0.1 Hz in the South. The general decrease of the fundamental resonance frequency from North to South is consistent with the geological structure of the basin, which shows an increase in the thickness of the Quaternary and Tertiary sedimentary cover towards the south (Bullen et al., 2001, their Figures 4 and 5). Considering the high value of the S-wave velocity characterizing the shallow Quaternary layers (Figure 8), the low value of the resonance frequency might be indicative of a deep impedance contrast, likely to exist between the Sharpyldak and Chu formations (Bullen et al., 2001). The lower-resonance frequencies observed in the south-western part of the area are consistent with a thickening of the sedimentary cover as proposed by Bullen et al. (2001) and in the references therein.

The seismic noise recorded at about 200 single station noise measurement points (SSNP) were also analyzed using HVSR technique. The fundamental resonance frequency estimate from the SSNP and temporary seismic network are plotted in Figure 4 using natural neighbor interpolation. Figure 4 shows the higher resonance frequency in the south towards the Kyrgyz Range, starting from 0.28 to higher than 1 Hz. The central part of the city shows lower resonance frequencies between 0.1 and 0.2 Hz, while the northern part towards Chu-Ili Mountain has resonance frequencies between 0.2 and 0.3 Hz.

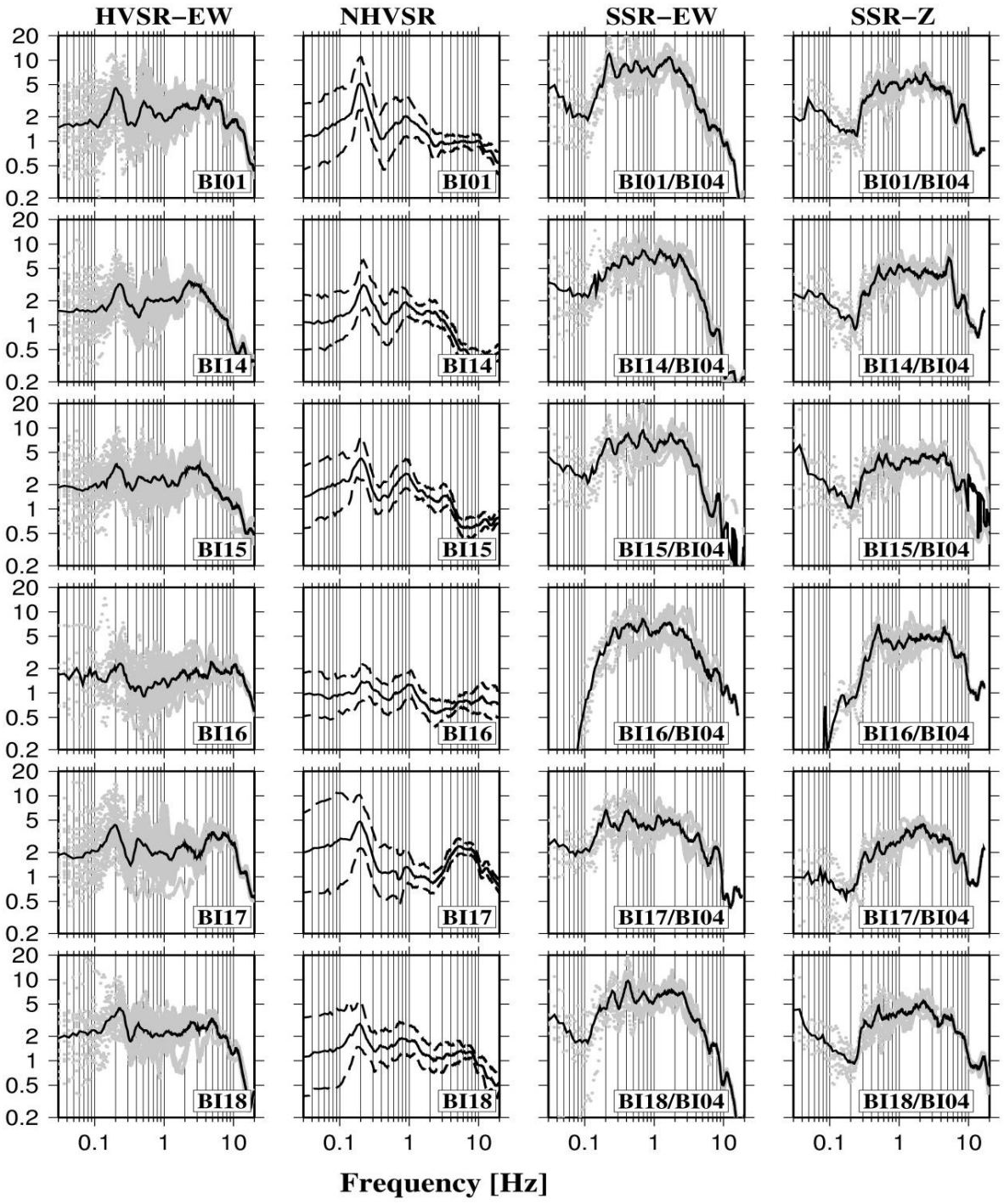

Figure 3: *Site amplification estimated at different stations using earthquake and seismic noise data. 1st column from left side, horizontal to vertical spectral ratios for earthquakes, second column, horizontal to vertical spectral ratios for the seismic noise, third column, standard spectral ratios for the horizontal component from earthquakes and last column is for standard spectral ratios for the vertical components of earthquake recordings (Parolai et al., 2010).*

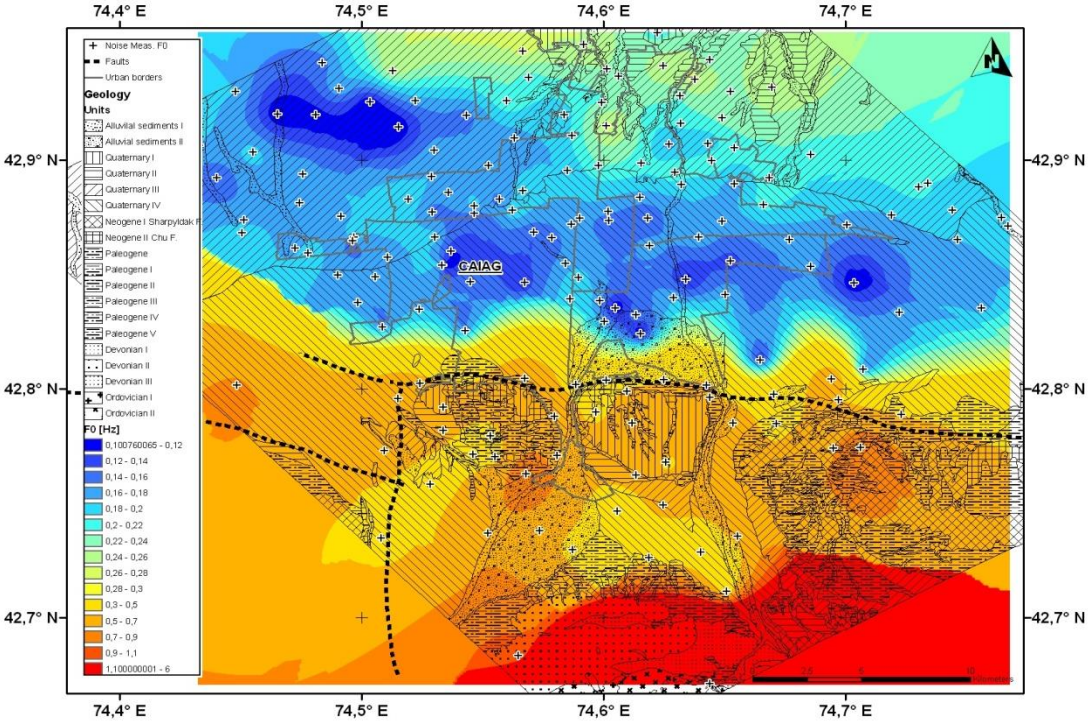

Figure 4: *Fundamental resonance frequency map of Bishkek (Kyrgyzstan). The crosses indicate sites where single station noise measurements were carried out.*

2.1.1 Improving the spatial resolution of ground motion variability in Bishkek using earthquake and seismic noise data

Using the K-means clustering algorithm, three clusters of site response types have been identified, based on their similarity of SSRs. The cluster's site responses were adopted for sites where only single station noise measurements were carried out, based on the results of correlation analysis. The spatial variability of the site response correlates well with the main geological features in the area. In particular, variability is noted from south to north, consistent with both the changes in the thickness of the sedimentary cover over the basin and in the Quaternary material outcropping at the surface. For a detail discussion of this topic, the reader is referred to Ullah et al. (2013).

Figure 5 shows the spatial distribution of stations over the geological map of Bishkek. The results from the stations are seen to mainly cluster into three groups. In the north towards the Chun-Ili Mountains, the site amplifications are higher, followed by a transition area with medium amplification and then lower amplification in the south towards the Kyrgyz Range. This distribution also follows the geological pattern and the depth distribution of different geological units as the spectral ratios reflect the deeper geological structure.

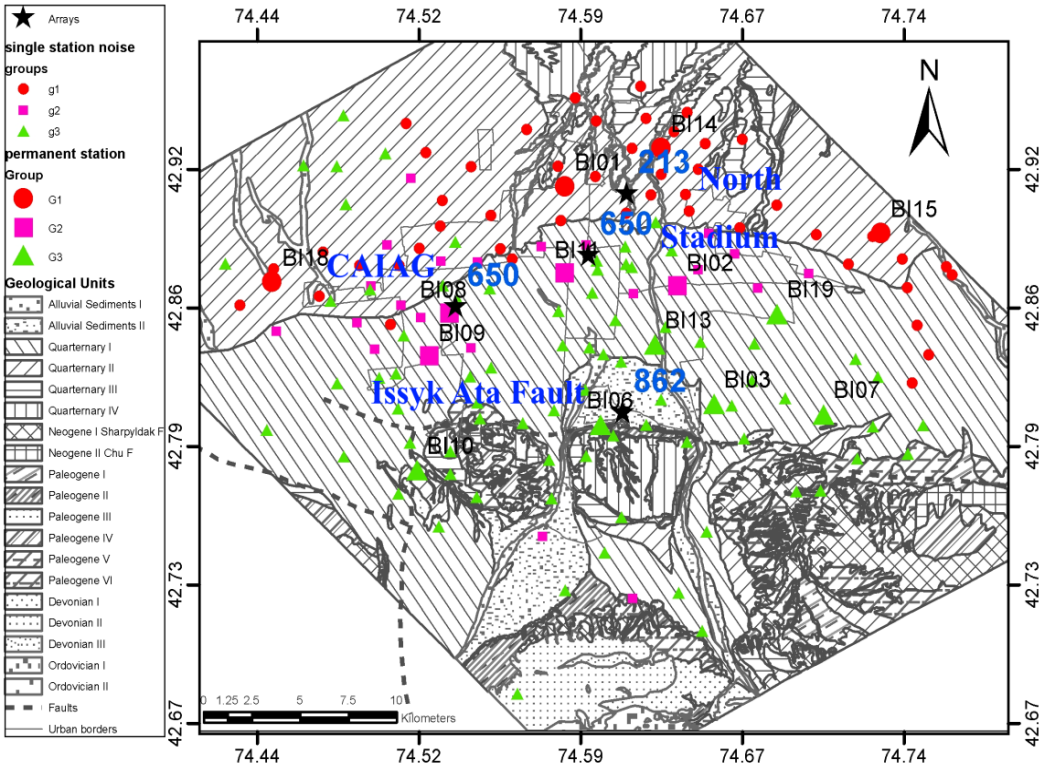

***Figure 5**: Map of the Bishkek area showing locations of measurement sites and surficial geology (see also Figure 1). The bigger size shapes indicates the permanent stations of temporary network, while the smaller sizes represent the noise recording stations at dense grid. Different colors represent the different clusters or groups after the clustering analyses. The stars with blue text show the location of array recordings with Vs30 values (Ullah et al., 2015).*

Figure 6 shows the site responses typically observed in each of the three identified cluster. The bold continuous line in each cluster represents the logarithmic average of that cluster. The grey area shows the frequency range where analyses are not considered because of the spectra ratios being affected by the site response at the reference site (see Parolai et al., 2010).

Figure 7 shows the spectral amplification over the study area from SSR at different frequencies. This figure is obtained by plotting the spectral ratios from SSR assigned to each seismic noise measurement location after the clustering and correlation analysis. The highest amplification of ground motion is observed at 0.4 Hz in the north, reaching about a factor of 10.

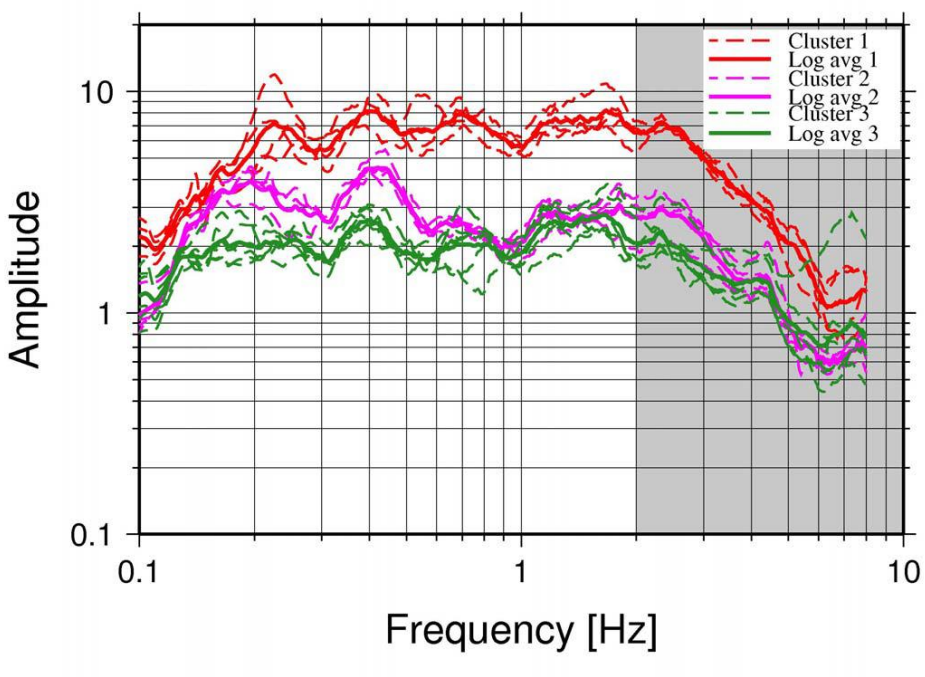

***Figure 6**: Logarithm average of the SSRs for the temporary stations. Different colors indicate the different clusters, while bold colors in each cluster show the logarithmic average of that cluster (see Figure 5). The grey area represents the frequency range where analyses are not considered due to the amplification at the reference site.*

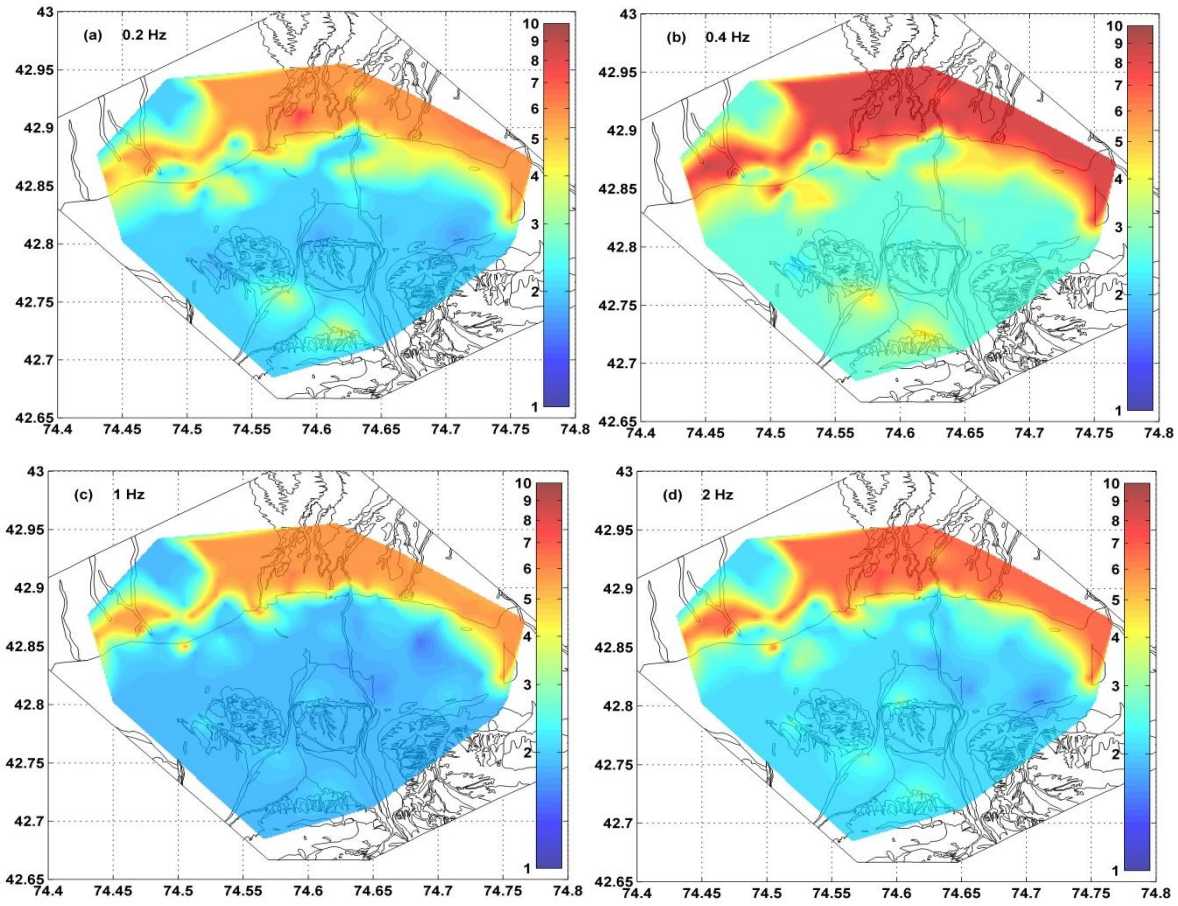

***Figure 7:** Spatial distribution of SSRs at selected frequencies (0.2, 0.4, 1 and 2 Hz) using Natural Neighbors Interpolation (Ullah et al., 2013).*

2.1.2 Seismic noise arrays

In Bishkek, seismic noise was also recorded using small arrays of stations in order to be able to estimate the S-wave velocity profile of the subsurface. Three locations (Figure 5) have been selected from south to north within the urban area. The results from the first one, at station BI08 (also indicated by the label CAIAG in Figure 5) are shown in Figure 8, which presents the dispersion curve obtained using the Extended Spatial Auto-Correlation (ESAC) method, and displays normal dispersive behavior between 3 and 13 Hz. This dispersion curve was inverted using simplified linear inversion to estimate the underlying S-wave velocity profile. The obtained profile shows a regular increase of velocity with the depth, starting from 600 m/s in the shallowest layers (0-25 m depth) and increasing to 1380 m/s in the deepest parts.

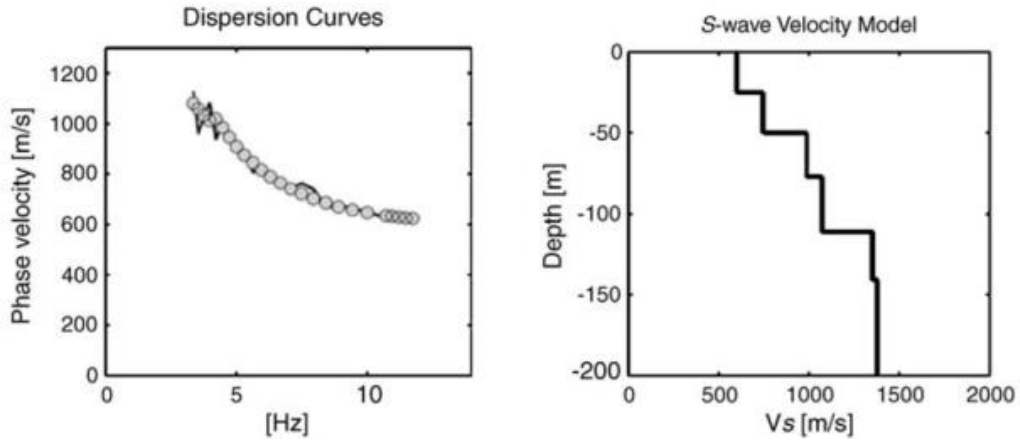

***Figure 8**: Results of the array analysis over site BI08 (CAIAG). Left side: observed (black line) and reconstructed (grey circles) dispersion curve. Right side: S-wave velocity model obtained by inverting the dispersion curve (Parolai et al., 2010).*

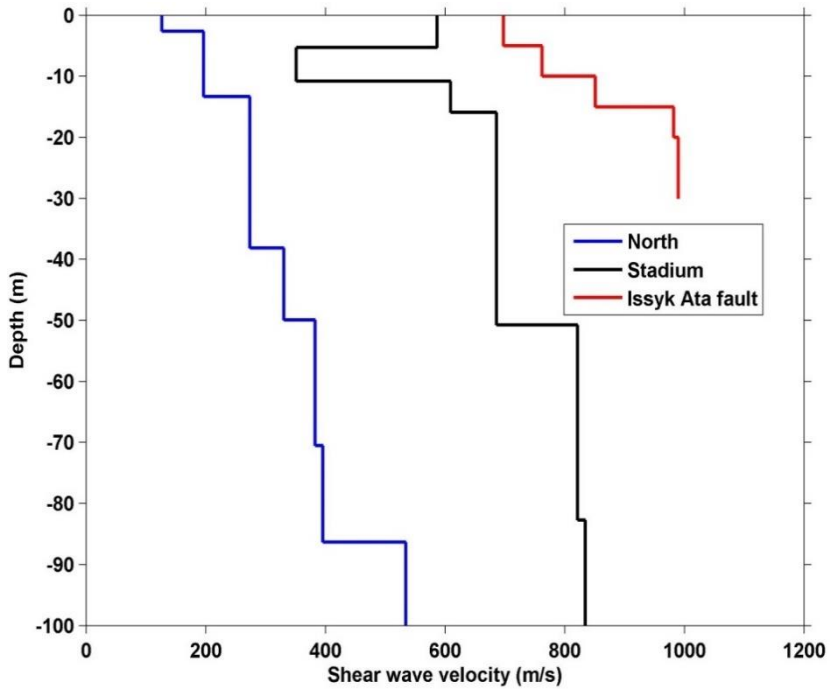

***Figure 9**: Results of array analyses in Bishkek at different locations (Figure 5, Ullah et al., 2015).*

The results of all the array analyses are shown in Figure 9. The highest shear wave velocity (about 862 m/s in the upper 30 meter) was observed in the southern-most array located close to the Issyk Ata fault. The lowest shear wave velocity, with an average shear wave velocity in the upper 30 meters of about 213 m/s, was estimated in the northern part of the city. These profiles are providing useful information that need to be considered for the probabilistic seismic hazard calculation.

2.2 Karakol

A temporary seismic network of 16 short period sensors, operating continuously from 10th of July 2011 until October 2011, was installed in the city of Karakol, eastern Kyrgyzstan. A large number of local, regional and tele-seismic events were recorded by the network, out of which 50 are used for site effects investigation since they had been recorded simultaneously by the maximum number of stations. Furthermore, single station seismic noise measurements (SSNM) were carried out at 34 sites across the city. Since the shear-wave velocity structure is not known below the city, 3 seismic noise array measurements with 20 stations were carried out in different areas of the city. Figure 10 shows the location of the stations composing the temporary seismic network, the SSNM and the array measurements. Station KA08 in the south-east of the city was used as a reference site.

Results from the SSR method (see the example depicted in Figure 11) show that in Karakol the amplification of ground motion (ranging from 2 to 9) occurs over a broad frequency range. Higher amplifications are found in the northern part of the city near the Lake Issyk-Kul. Note that the amplification also affects frequencies as low as 0.2 and 0.3 Hz.

In general, the frequency of the peaks of amplification was found to be consistent when comparing the results from earthquake H/V and SSR, however, at some sites, the earthquake H/V provides lower amplification than the SSR.

Figure 11 shows SSR and the noise H/V results spectral ratios for a station, KA02, in the middle of the city. A broad but moderate amplification is observed on the SSR results of station KA07, affecting also the vertical component of ground motion. The noise H/V ratio show always lower amplification levels, but with a clear peak around 4 Hz. This peak is also observed in the SSR, and might indicate the existence of a vertical heterogeneity in the shallow layers. It should be noted that the observed difference in amplification between the two horizontal components of ground motion may, together with the broad band amplification and the differences between SSR and H/V, suggest a very complex subsoil geometry, leading to 2D and 3D site effects.

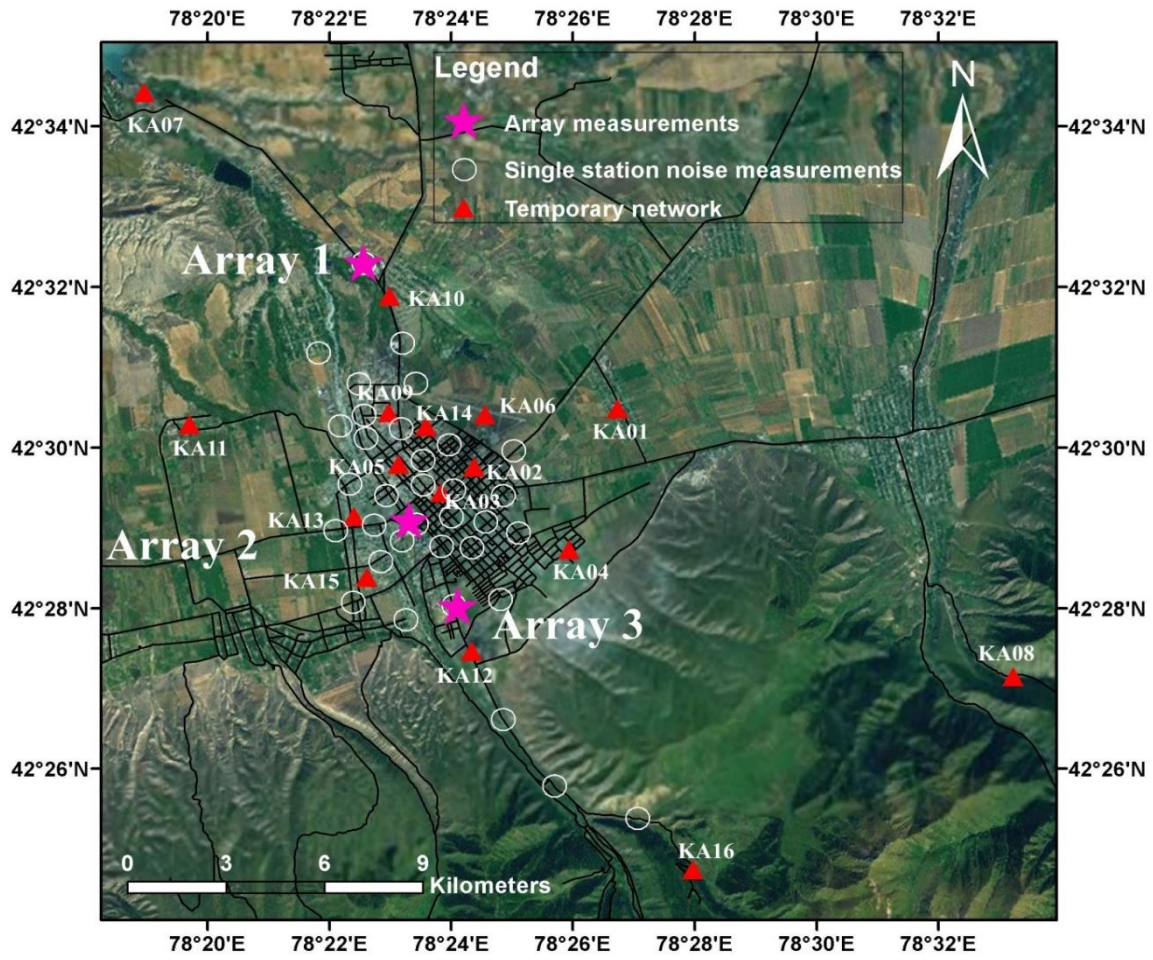

***Figure 10**: Location of the temporary seismic network in Karakol. Different objects are shown in the legend.*

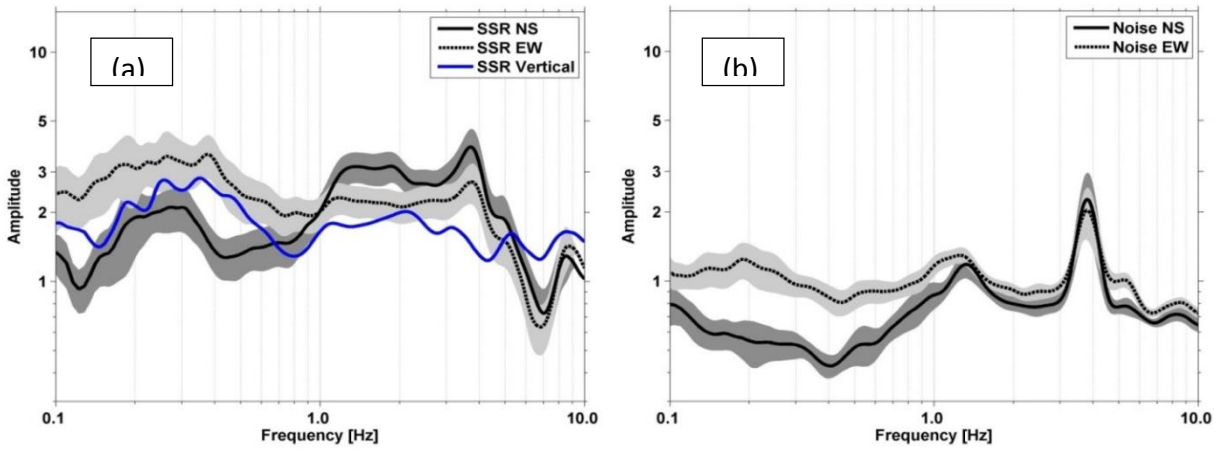

***Figure 11:** Spectral ratios for station KA02 using different components and methods. (a) Site amplification using SSR method for the S-wave window of earthquake records. (b) Site amplification using H/V spectral ratio method. The grey color indicates ± 1 standard deviation.*

Figure 12 shows the spectral ratios for different components using SSR for earthquakes and H/V for noise recordings for station KA07 in the northern part of the city near Lake Issyk-Kul. This station shows the largest amplification from earthquake records with values as large as a factor of 10. Also, the amplification starts from frequencies as low as 0.1 Hz up to 10 Hz, with an average amplification about 5. The different components show different amplification between 0.5 and 2 Hz. However, the H/V for noise shows very low amplification in the lower frequencies and a de-amplification over the higher frequencies, suggesting amplification of the vertical component. Also, there is no observation of a clear peak, which might be indicative of low impedance contrasts between the bedrock and overlying sediments.

Figure 13 shows the results of the array analyses for different location in the city. Array 1, which is located in the northern part of the city near Lake Issyk-Kul shows the lowest shear wave velocity, with values as low as 200 m/s near the surface. Arrays 2 and 3, which are located near the center of the city, show almost the same shear wave velocity, about 300 m/s, near the surface. This is consistent with the amplification observed from the SSR and H/V.

Figure 14 shows the resonance frequency map of Karakol obtained from the analyses of single station noise measurement points in the city. It is seen that across the city there is a very low resonance frequency. The southern part shows a frequency about 0.4 Hz with the highest about 0.67 Hz near the center of the city.

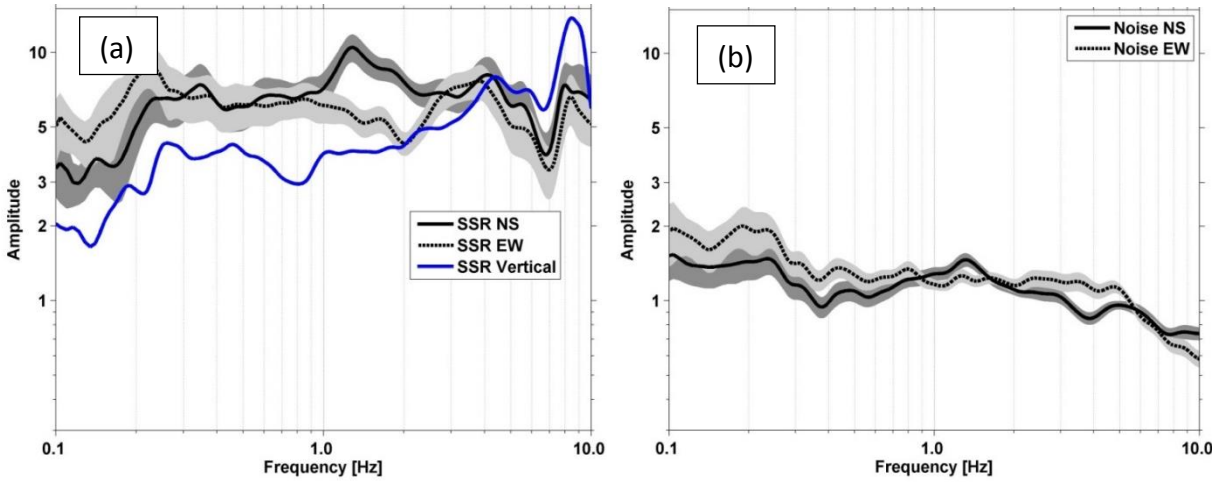

Figure 12: *Site amplification for station KA07 in the northern part of the city near Lake Issyk-Kul, using different components and methods. (a) Site amplification from using SSR method. (b) Site amplification using H/V spectral ratio method. The grey color indicates ± 1 standard deviation.*

The analysis of site effects using different methods show the largest site amplification in Karakol in the north near Lake Issyk-Kul. The difference in amplification using different components of ground motion suggests a strong lateral heterogeneity of the deeper structure. Based on the resonance frequency obtained by the single station noise measurements and the shear wave velocity structure obtained by the array analyses, it is expected that the bedrock is located deeper than 500 meters.

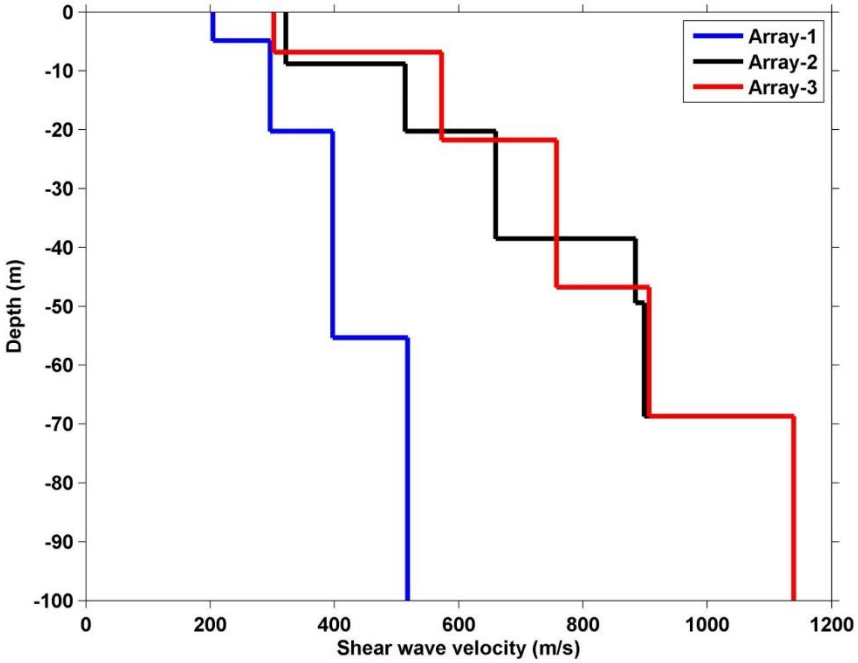

***Figure 13**: Results of array analyses in Karakol at different locations as shown in Figure 10.*

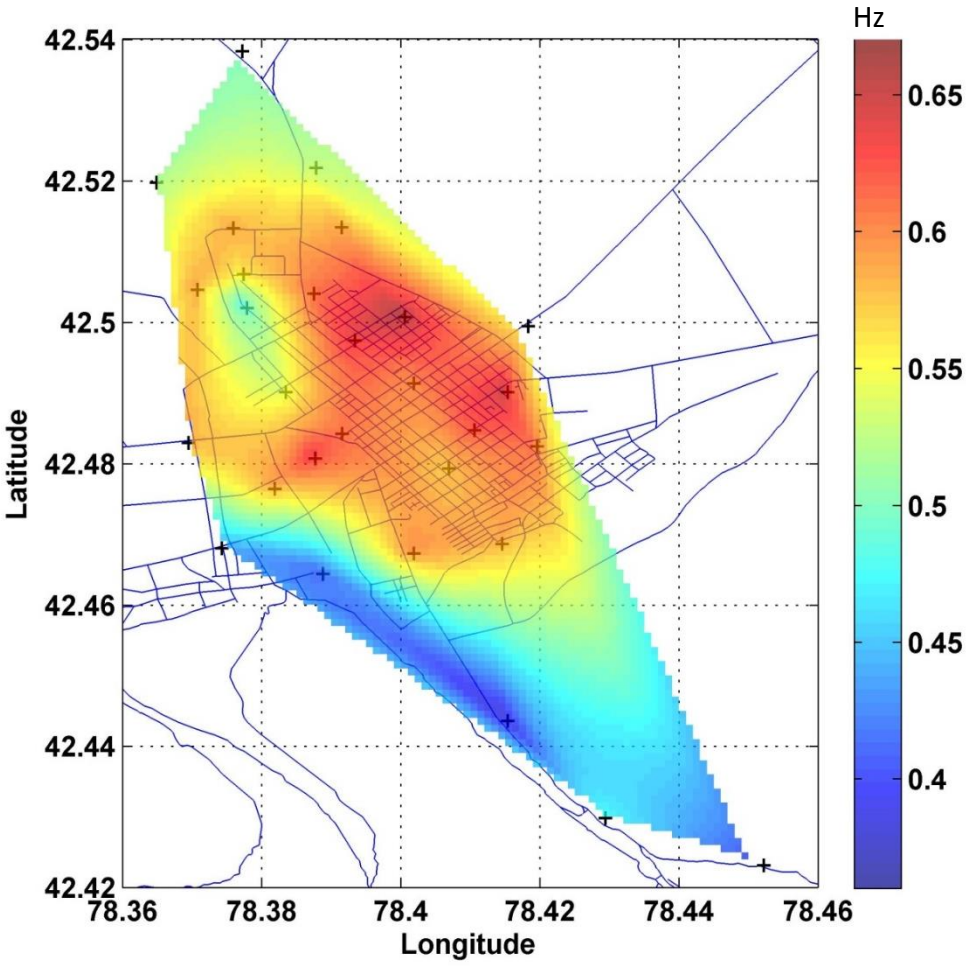

***Figure 14:** Resonance frequency map of Karakol estimated from the H/V spectral ratios of noise.*

3 Integration of site effects into PSHA for Bishkek

Although the variability in the surface geology potentially leads to the modification of earthquake-induced ground motion over short distances, it is very often not appropriately accounted for when considering seismic hazard assessment at the urban level. For Bishkek, the influence of geological structure on the seismic hazard assessment is considered using different proxies for the site effects. This includes the shear wave velocity and the response spectral ratios.

In order to carry out the seismic hazard assessment for Bishkek, the areal sources are taken from the regional hazard model for Central Asia (Ullah et al., 2015), including those that are only partly within a buffer distance of 200 km from the center of the city. These sources are designed mainly based on the crustal seismicity distribution, considering events with hypocentral depths less than 50 km. The earthquake catalog used was compiled after having converted the original magnitudes of the events to a common Moment magnitude Mw. Figure 15 shows the location of the area source model for Bishkek along with a buffer distance around the city.

Site effects are accounted for in the PSHA by considering them directly in the ground motion prediction equation (GMPE) via the Vs30 values estimated at each site (based on the array measurements presented in section 2.1.2) and the response spectra amplification factors, estimated by considering the empirical site responses derived for Bishkek (section 2.1). Please note that Vs30 refers to the average S-wave velocity in the uppermost 30 m. More details are reported in Ullah et al. (2015). The Boore and Atkinson (2008) GMPE is used in this study, since 1) no data are available for an ad-hoc calibration or selection of any existing relationships and 2) it is recommended by GEM for active shallow crust conditions.

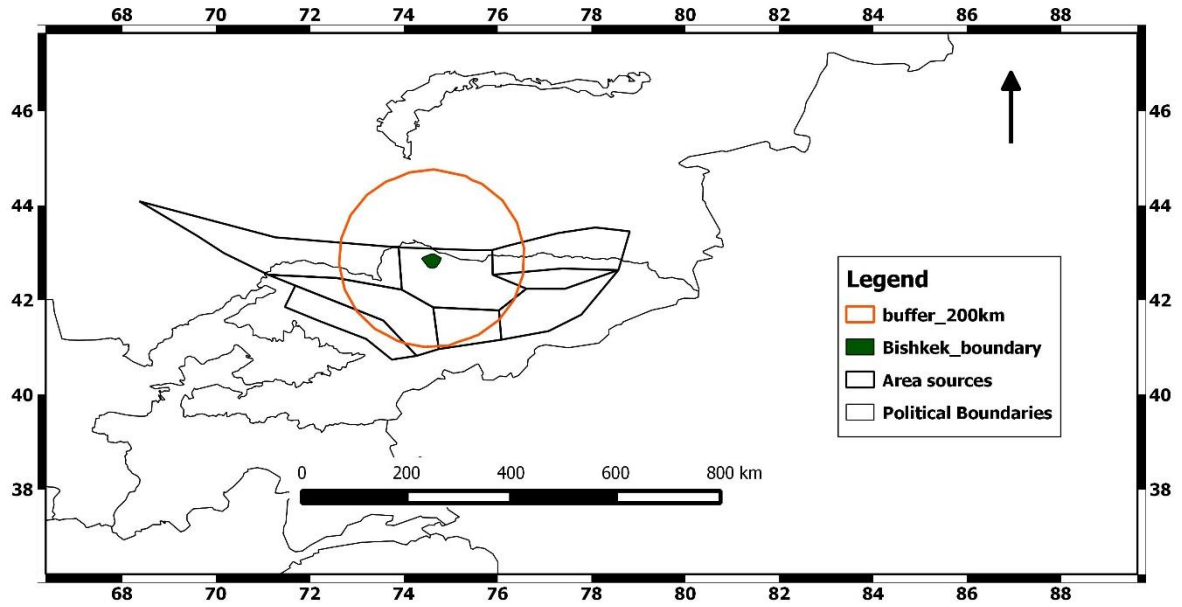

***Figure 15**: Area source model for Bishkek. The area sources are taken from the EMCA model for the region (Ullah et al., 2015).*

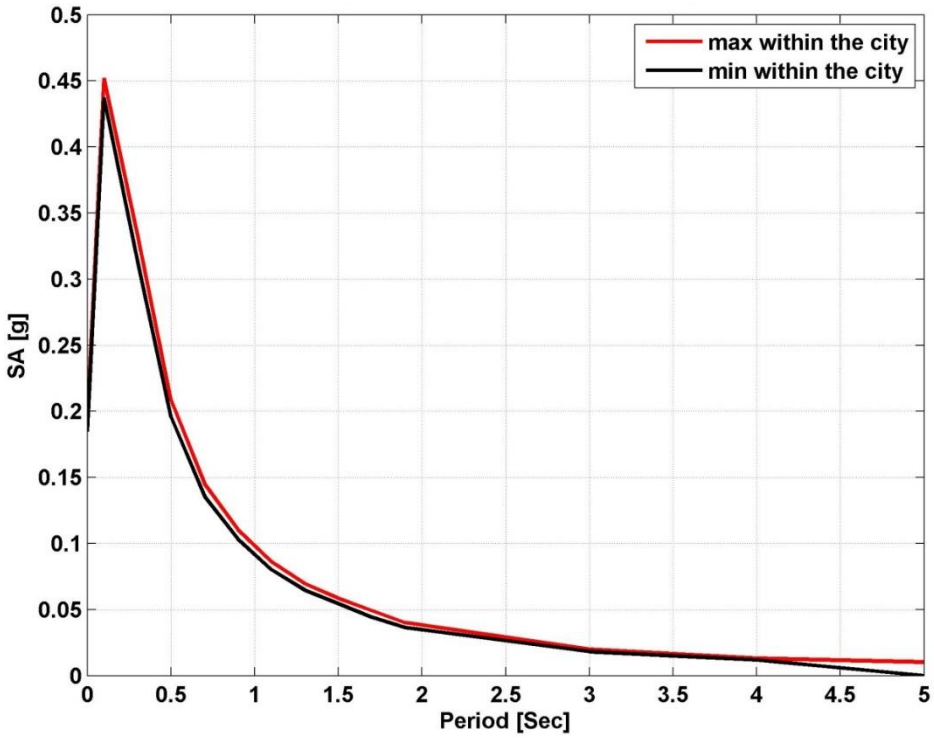

Figure 16: *Estimated seismic hazard variation within the city of Bishkek for rock-site conditions (Vs30=900m/s), for a 10% probability of exceedance over 50 years.*

Figure 16 shows the maximum and minimum values of the Spectral Acceleration (SA) with a 10% probability of exceedance over 50 years, obtained in different localities when considering a uniform rock site conditions for the area of Bishkek. The values are very close, showing that when site effects are not accounted for, the level of hazard shows little small spatial variability. Furthermore, in this case only a slight increase in the expected ground motion from north to south is observed (Figure 17), very likely related to the dominance of the shaking produced by the larger number of earthquake sources in the south. The largest hazard observed for this model is represented by a SA of 0.45 g at 0.1s (10 Hz) and a PGA reaching 0.21 g in the southern outskirts of the city.

Figure 18 again shows the maximum and minimum values of SA with 10% probability of exceedance over 50 years, but this time including the variability associated with Vs30. The maximum hazard values found in this case are 0.64 g for the SA at 0.3 s and 0.31 g for the PGA. Note that differently from what was obtained when only rock-site conditions are considered, the largest values are found in the northernmost area of the city (Figure 19). This is the area where, due to the low S-wave velocities, the highest amplification of ground motion is estimated to occur.

Similar trends in the results are observed when site effects are accounted for through the response spectra ratio coefficients calculated using the estimated empirical site responses. That is, the minimum and maximum SA curves show (Figure 20) larger values than those calculated for rock site conditions (Figure 16) and the area affected by the largest hazard becomes the northernmost one (Figure 21). However, in this case, the maximum hazard calculated for SA at 0.5s reaches values up to 1.13g, much larger than that obtained by considering

Vs30 only. It should be noted that, owing to the amplification at the reference station above 2 Hz, calculations for shorter periods below 5s (above 2 Hz) are not carried out. In any case, based on these results, it should be remarked that these values, when extrapolated to a first order for the PGA are of the same order of magnitude to what could be estimated by converting the intensities of the old Bishkek micro-zonation maps in PGA using empirical regressions such as those of Ulomov (1999).

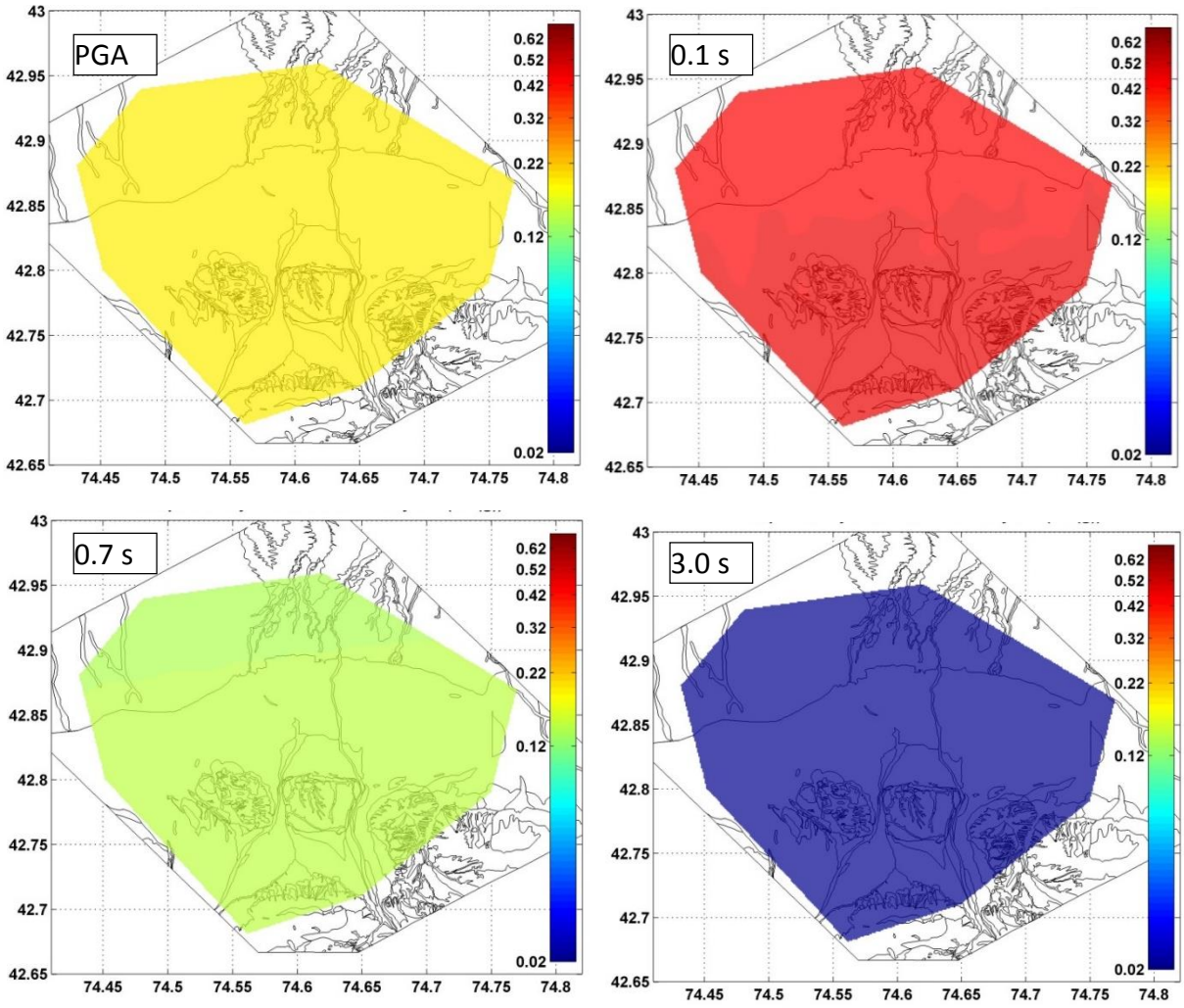

Figure 17: *Seismic hazard in terms of 10% probability of exceedance over 50 years for rock-site conditions. The hazard is shown for PGA and spectral acceleration at different selected periods in terms of g.*

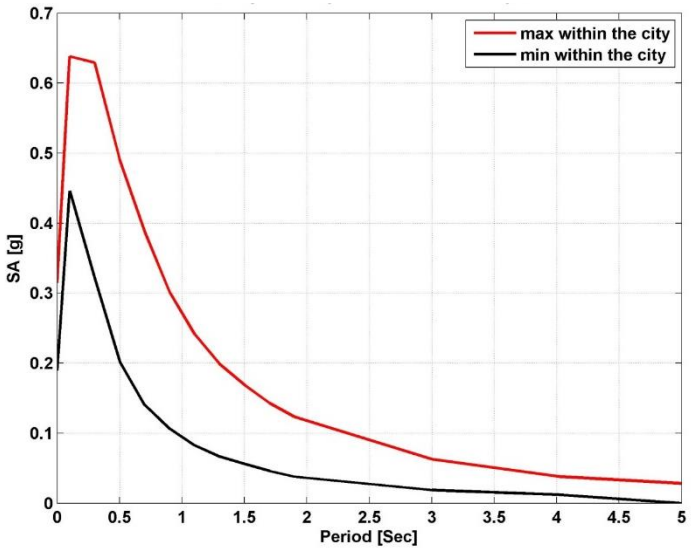

Figure 18: *Estimated seismic hazard variations within the city of Bishkek considering site effects based on Vs30 variations, for a 10% probability of exceedance over 50 years.*

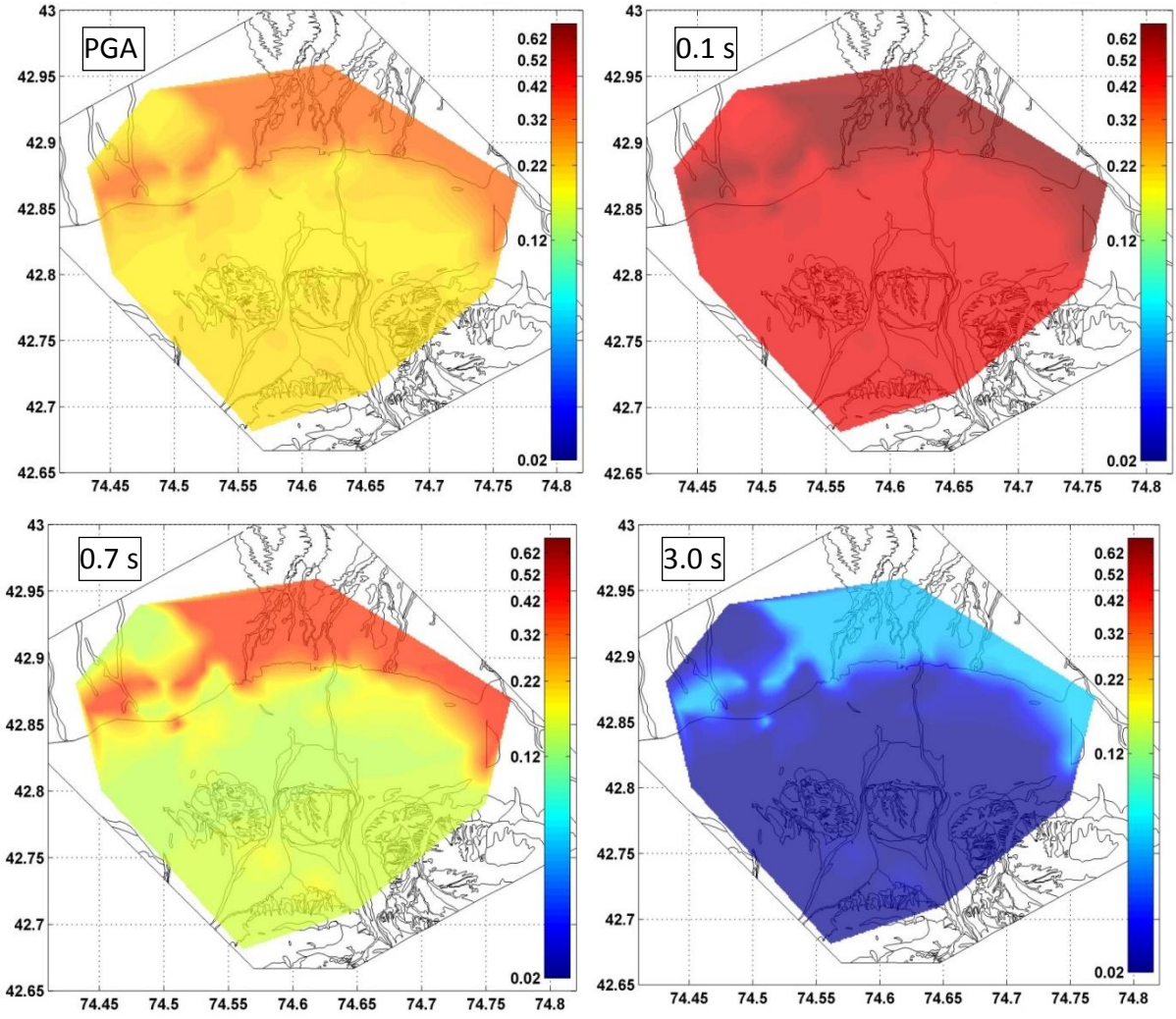

Figure 19: *Estimated hazard for a 10% probability of exceedance in 50 years considering the distribution of Vs30 values. The level of hazard is shown for PGA and spectral acceleration at diff. selected periods of g.*

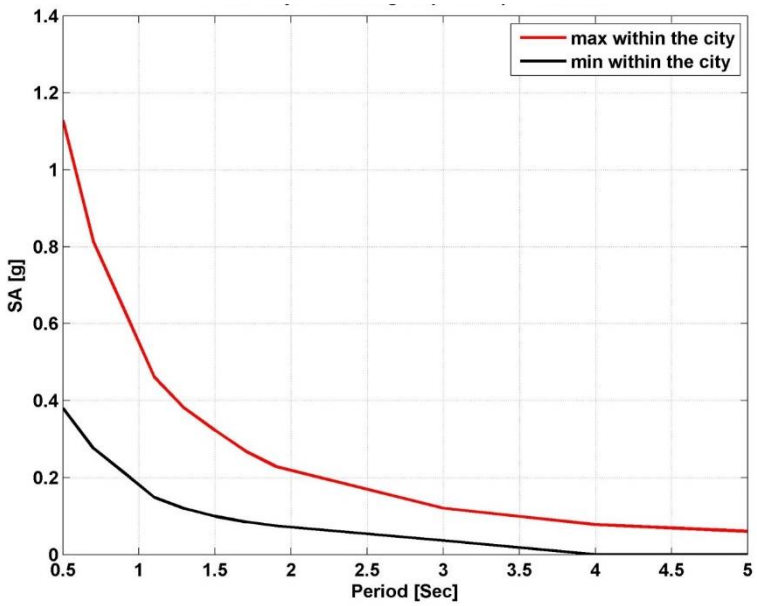

Figure 20: *Estimated seismic hazard variations within the city of Bishkek considering site effects estimated from response spectrum ratios, for a 10% probability of exceedance over 50 years.*

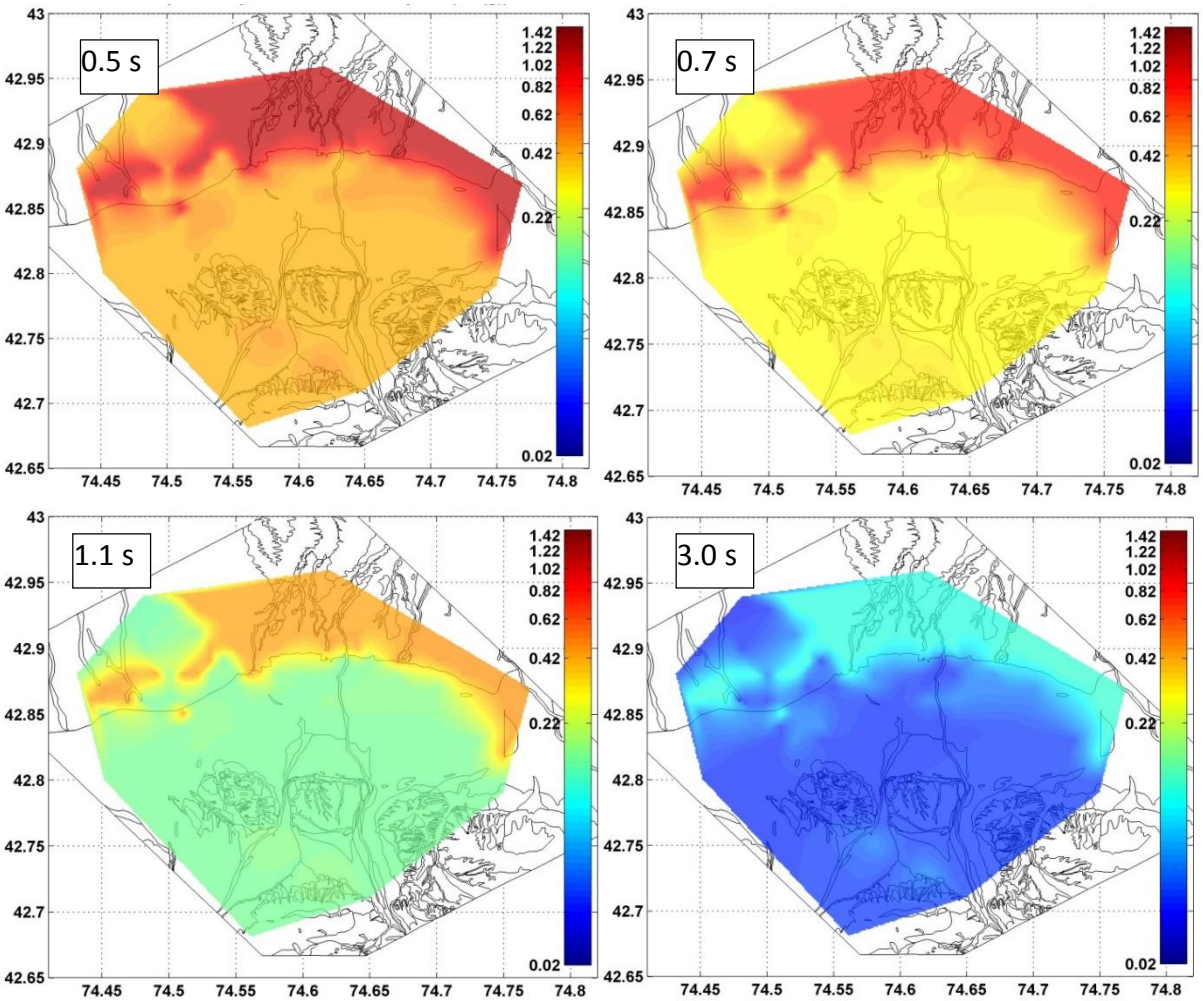

Figure 21: *Estimated hazard for 10% probability of exceedance over 50 years considering site effects in terms of response spectrum ratios for different spectral periods.*

4 Conclusions and final comments

With regards to the different methodologies used for site assessment in Bishkek, we find that although the NHVSR (Noise Horizontal to Vertical Spectral Ratio) shape, especially at intermediate frequencies, might be different from the SSR (Standard Spectral Ratio) gained from the same station, their variability is consistent with that of the SSR. Therefore, although seismic noise cannot be used to estimate directly the site response of the site, it is a useful tool, when combined with a limited number of temporary station earthquake recordings, to improve the spatial resolution of the site response variability.

Introducing site effects into the seismic hazard assessment of Bishkek changes the orientation of the estimated hazard trend with respect to rock site conditions, which assumed homogeneous Vs30 values over the whole urban area. For the rock site condition, the southern part of Bishkek has the highest hazard, with a slight decrease of hazard towards northern part of the city. The maximum hazard observed for Bishkek considering rock site conditions is 0.21 g PGA, with 0.45 g spectral acceleration at 0.1 s in the southern part of the city for a return period of 475 years. However, including site effects into the hazard analysis inverts the trend of hazard in the city. Using the Vs30 values, the maximum hazard is observed at 0.3 s, having 0.64 g spectral acceleration with 0.31 g PGA in the northern part of the city for a 475 years return period. For the response spectral ratios, the maximum hazard is calculated for spectral acceleration at 0.5 s reaching up to 1.13 g for a 475 years return period. Using response spectral ratios and Vs30 as proxies for site effect shows not only the importance of including site effects in hazard studies, but also shows the importance of selecting the proper proxy. In particular, the Vs30 might not be the most appropriate proxy for large basins, like the Chu one, where the effect of intermediate to long-period waves become more important, which might lead to the underestimation of ground motion. On the other hand, considering response spectral ratios as a proxy for site effects estimated from weak motion data might not be an appropriate for sites having large seismicity, potentially leading to an overestimation of the ground motion since it is not accounting for the soil's nonlinear behavior. While this might be a relatively minor problem in the southern parts of the city where the soil mainly consists of boulders and pebbles grading slowly to gravel toward the center of the urban area, it can be a problem for the northernmost part of Bishkek where silty deposit and loess prevail.

Further studies should also be carried out to account for possible nonlinear soil behavior and liquefaction.

5 References

Boore, D. M. and G. M. Atkinson (2008), Ground-motion prediction equations for the average horizontal component of PGA, PGV, and 5%-Damped PSA at spectral periods between 0.01s and 10.0s. Earthquake Spectra, vol. 24(1), pp. 99-138. http://doi.org/10.1193/1.2830434.

Bormann, P. (Ed.) (2012). New Manual of Seismological Observatory Practice (NMSOP-2), IASPEI, GFZ German Research Centre for Geosciences, Potsdam; http://nmsop.gfz-potsdam.de; http://doi.org/10.2312/GFZ.NMSOP-2.

Bullen, M. E., Burbank, D. W., Garver, J. J. and Abdrakhmatov, K. Y. (2001) Late Cenozoic tectonic evolution of the northwestern Tien Shan: New age estimates for the initiation of mountain building. Geological Society of America Bulletin, vol. 113(12), pp. 1544–1559. http://doi.org/10.1130/0016-7606(2001)113<1544:LCTEOT>2.0.CO;2.

Parolai, S., Orunbaev, S., Bindo, D., Strollo, A., Usupaev, S., Picozzi, M., Di Giacomo, D., Augliera, P., D'Alema, E., Milkereit, C., Moldobekov, B. and Zschau, J. (2010) Site effects assessment in Bishkek (Kyrgyzstan) using earthquake and noise recording data. Bulletin of the Seismological Society of America, vol. 100(6), pp. 3068-3082, http://doi.org/10.1785/0120100044.

Parolai, S. and Richwalski, S. M. (2004) The importance of converted waves in comparing H/V and RSM site response estimates, Bulletin of the Seismological Society of America, vol. 94(1), pp. 304-313. http://doi.org/10.1785/0120030013.

Pilz, M., Abakanov, T., Abdrakhmatov, K., Bind, D., Boxberger, T., Moldobekiv, B., Orunbaev, S., Silacheva, N., Ullah, S., Usupaev, S., Yasunov, P. and Parolai, S. (2015) An overview on the seismic microzonation and site effects studies in Central Asia. Annals of Geophysics, vol. 58(1), S0104, http://doi.org/10.4401/ag-6662.

Strollo, A., Parolai S, Jäckel, K. H., Marzorati, S. and Bindi, D. (2008) Suitability of Short-Period Sensors for Retrieving Reliable H/V Peaks for Frequencies Less Than 1 Hz. Bulletin of the Seismological Society of America. vol. 98(2), pp. 671-681, http://doi.org/10.1785/0120070055.

Takahashi, K., Ohno, S., Takemura, M., Ohta, T., Sugawara, Y., Hatori, T. and Omote, S. (1992) Observation of earthquake strong motion with deep borehole: Generation of vertical motion propagating in surface layers after S arrival. Proceedings of the 10th World Conference on Earthquake Engineering, vol. 3, pp. 1245-1250.

Ullah, S., Bindi, D., Pittore, M., Pilz, M., Orunbaev, S., Moldobekov, B. and Parolai, S. (2013) Improving the spatial resolution of ground motion variability using earthquake and seismic noise data: the example of Bishkek (Kyrgyzstan). Bulletin of Earthquake Engineering, vol. 11(2), pp. 385-399, http://doi.org/10.1007/s10518-012-9401-8.

Ullah, S., Bindi, D., Pilz, M. and Parolai, S. (2015) Probabilistic Seismic hazard assessment of Bishkek, Kyrgyzstan, considering empirically estimated site effects. Annals of Geophysics, vol. 58(1), S0105, http://doi.org/10.4401/ag-6682.

Ulomov, V.I (1999) Seismic hazard of Northern Eurasia. Annals of Geophysics, vol. 52(6), pp. 1023-1038, http://doi.org/10.4401/ag-3785.

6 Recent articles about site effects in Central Asia and the Kyrgyz Republic

Parolai, S., Orunbaev, S., Bindi, D., Strollo, A., Usupaev, S., Picozzi, M., Di Giacomo, D., Augliera, P., D'Alema, E., Milkereit, C., Moldobekov, B. and Zschau, J. (2010) Site effects assessment in Bishkek (Kyrgyzstan) using earthquake and noise recording data. Bulletin of the Seismological Society of America, vol. 100(6), pp. 3068-3082, http://doi.org/10.1785/0120100044.

Pilz, M., Abakanov, T., Abdrakhmatov, K., Bind, D., Boxberger, T., Moldobekiv, B., Orunbaev, S., Silacheva, N., Ullah, S., Usupaev, S., Yasunov, P. and Parolai, S. (2015) An overview on the seismic microzonation and site effects studies in Central Asia. Annals of Geophysics, vol. 58(1), S0104, http://doi.org/10.4401/ag-6662.

Ullah, S., Bindi, D., Pittore, M., Pilz, M., Orunbaev, S., Moldobekov, B. and Parolai, S. (2013) Improving the spatial resolution of ground motion variability using earthquake and seismic noise data: the example of Bishkek (Kyrgyzstan). Bulletin of Earthquake Engineering, vol. 11(2), pp. 385-399, http://doi.org/10.1007/s10518-012-9401-8.

Ullah, S., Bindi, D., Pilz, M. and Parolai, S. (2015) Probabilistic Seismic hazard assessment of Bishkek, Kyrgyzstan, considering empirically estimated site effects. Annals of Geophysics, vol. 58 (1), S0105, http://doi.org/10.4401/ag-6682.

ISSN 2190-7110